ARRESTING FATIGUE CRACK IN COMPOSITE BONDED JOINT USING INTERLOCKED FIBER FEATURE

S. Minakuchi and N. Takeda

Graduate School of Frontier Sciences, The University of Tokyo
5-1-5 Kashiwanoha, Kashiwa-shi, Chiba 277-8561, JAPAN
Email: minakuchi@smart.k.u-tokyo.ac.jp

Keywords: Boltless structure, Bonded joint, Damage tolerance, Crack arrester, Fatigue test, FEA

ABSTRACT

Development of new design features that stop cracks from growing above a critical size is one of the key steps to realization of boltless composite structures. The authors have proposed a fiber-reinforcement-based concept that introduces continuous fibers in the adhesive layer and suppresses the crack propagation using massive fiber bridging. Following the previous study evaluating the arrester performance under mode-I and mode-II static loading conditions, this current study conducts crack lap shear (CLS) fatigue tests to evaluate the performance under a realistic condition. In addition, the arresting mechanism is clarified using finite element analysis.

1 INTRODUCTION

Bonded joints potentially possess clear advantages over traditional bolted joints. It significantly reduces the manufacturing cost related to drilling, fastening, and lightning protection. Furthermore, it allows more efficient load path with reduced component thickness and eliminates stress concentration around bolt holes. In spite of these advantages in terms of cost, weight, and performance, composite primary structures in aircraft are currently assembled with several hundreds of thousands of bolts. This is because existing bonding technologies and related non-destructive inspection techniques are unreliable (e.g., weak-bond detection is practically impossible) and cannot satisfy airworthiness requirements. Currently, mechanical fastening is required even in bonded areas so that the joints can maintain the limit load capability under the condition of global bondline failure. It is recognized that development of new design features that stop cracks from growing above a critical size is one of the key steps to realization of boltless structures [1].

Our previous study proposed a new crack arrester concept based on fiber-reinforcement [2]. The basic idea is that continuous high-strength fibers are introduced in the adhesive layer and their massive bridging suppresses crack propagation. One example is depicted in Fig. 1. This x-type crack arrester consists of 0° and 90° composite layers cured during the bonding process. The 90° layer is inserted between the 0° layers that are interlocked during the layup process. When a crack including the one propagating in the adherend approaches the arrester, the crack is robustly entrapped in the arrester by employing the surface feature of the adherends. When the crack passes through the crossing part, one 0° layer bridges the crack and suppresses the crack opening (Fig. 1 A). Furthermore, the 90° layer, which is constrained by the other side 0° layer, prevents the bridging layer from peeling off (Fig. 1 B). So when the crack further propagates, fibers break in the 0° and/or 90° layer and significant energy is absorbed.

Following the previous study evaluating the arrester performance under mode-I and mode-II loading conditions [2, 3], this current study conducts crack lap shear (CLS) fatigue tests to evaluate its performance under a realistic condition. CLS testing simulates a loading condition near stiffener run-out and mixed-mode crack propagation is induced [4]. In addition, finite element analysis is conducted to understand the crack arresting mechanism.

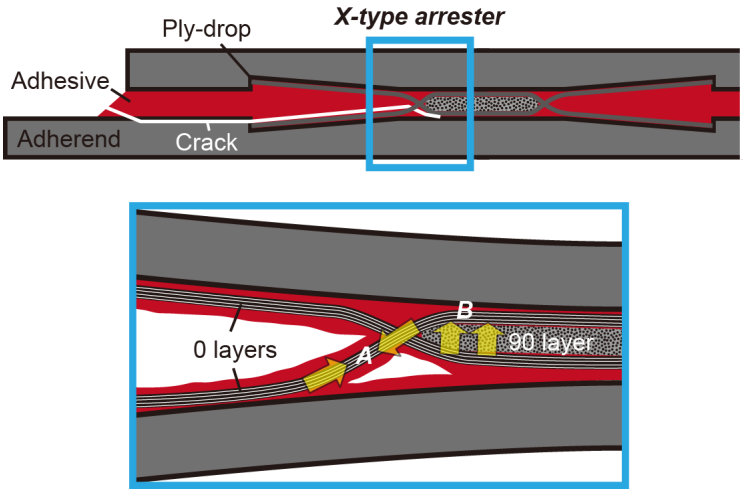

Figure 1: X-type arrester.

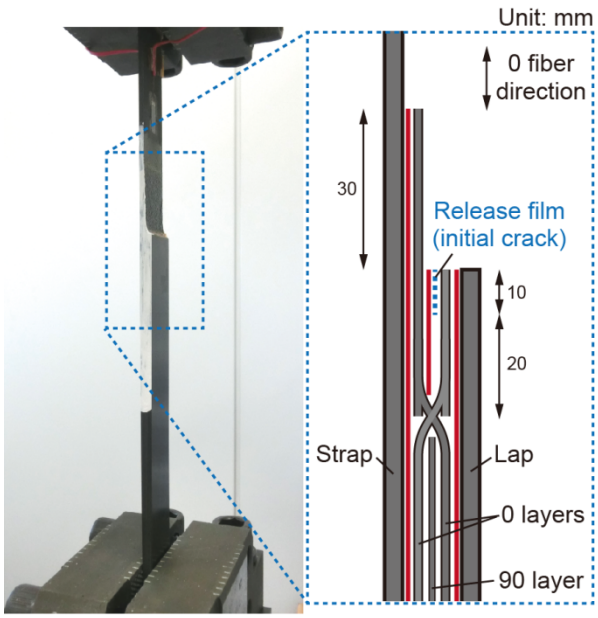

Figure 2: CLS test and lap edge configuration.

2 CRACK LAP SHEAR FATIGUE TEST

2.1 Materials and methods

CLS test setup is presented in Fig. 2. The specimen total length was 320mm and the width was 25mm. The adherends were quasi-isotropic carbon/epoxy laminates (T700S/2592, Toray, $[0/45/90/-45]_{2S}$, thickness 2.2mm) and the same carbon/epoxy prepreg sheets were used for the arrester. Two CLS test specimens with different arrester configurations were tested to clarify the effect of arrester thickness on crack stopping performance. The first specimen, 0-1_90-1, used one ply of the prepreg for both of the 0° and 90° layers. Meanwhile, the second specimen, 0-3_90-2, used three plies for the 0° layer and two plies for the 90° layer. The enlarged schematic view of the lap edge part is illustrated in Fig. 2. An initial crack was introduced at the lap edge, simulating the situation that the crack was entrapped in the arrester. So this current study evaluated the arrester performance by focusing on the crack stopping at the crossing part. First, the carbon/epoxy prepreg sheets for the 0° layers of the arrester were slit at intervals of 5 mm and interlocked as depicted in Fig. 3 (a). The non-crossing parts

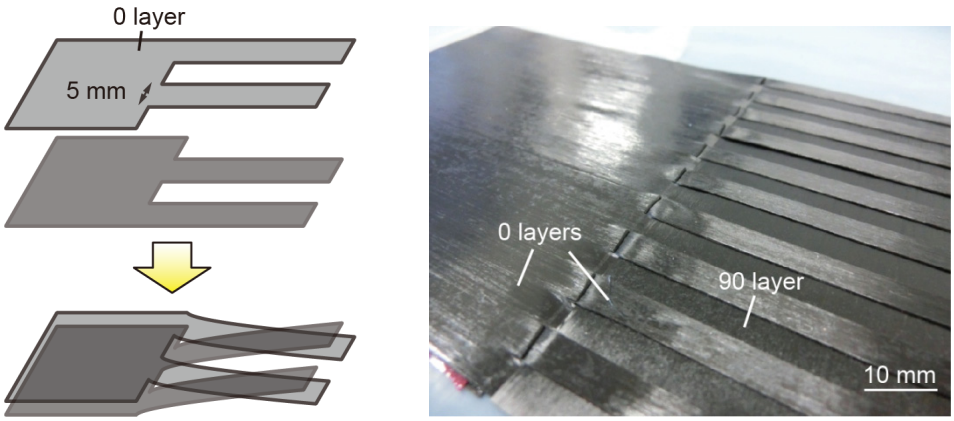

(a) Interlocking process of 0° layers. (b) Stacked arrester.

Figure 3: Preparation of arrester [2].

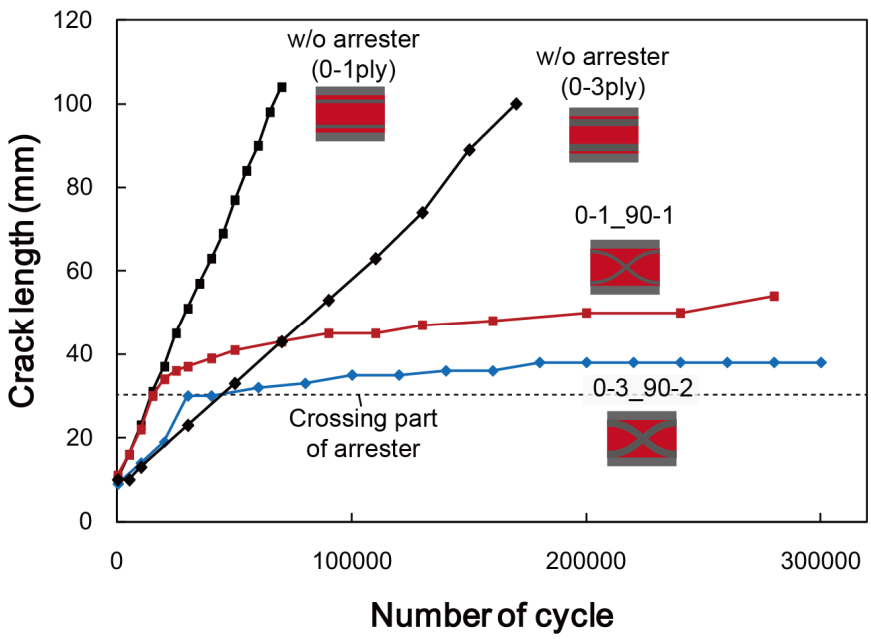

Figure 4: Fatigue crack growth curves obtained.

were removed. The 90° layer was then inserted between the 0° layers, Fig. 3 (b). Finally, the stacked prepreg sheets and epoxy-based adhesive films (FM300-2M, CYTEC SOLVAY GROUP.) were sandwiched between the adherends after removal of the surface peel plies and cured in an autoclave. The CLS fatigue tests were conducted using a servo-hydraulic test machine (Servopulser EHF-EB5 (Shimadzu)) at 8Hz sinusoidal with a load ratio R of 0.1 (tension-tension loading). The maximum load was 15kN that corresponded to the strap strain of 5400με. Additionally specimens without the arrester were fabricated by simply introducing one ply or three plies of 0° layers in the adhesive layer and tested for comparison.

2.2 Results

Figure 4 shows the fatigue crack growth curves obtained in the CLS tests. In the specimens without the arrester, cracks propagated with constant growth rates until the length reached 100mm. The growth rate depended on the amount of the 0° layer introduced in the adhesive layer because the 0° layer

reinforced the strap part and the strain at the crack tip was reduced depending on the thickness of the 0° layer. Meanwhile, the specimens with the arrester exhibited almost the same crack propagation behavior at the beginning of the tests as the specimens without the arrester, however the crack growth rate decreased when the crack tip passed through the crossing part of the arrester (i.e., crack length of 30mm). The deformation of the specimens was visually checked and it was confirmed that the crack opening was significantly suppressed and the crack propagated under the mode-II loading condition. In Specimen 0-1_90-1, the crack growth rate gradually decreased after the crack tip passed through the crossing part of the arrester and the crack propagated at a quite slow constant rate after the crack length exceeded 40mm. In contrast, in Specimen 0-3_90-2, the crack grow rate dramatically decreased as the crack tip reached the crossing part of the arrester and the crack stopped before its length reached 40mm. This result suggests that as the arrester thickness increases the crack growth rate decreases and the crack length at which the arresting effect becomes significant changes. After the CLS tests, one section including the crossing part of the arrester was cut out from Specimen 0-3_90-2 and observed by X-ray CT. The obtained 3D image is presented in Fig. 5. At the crossing part (cross-section A), the crack propagated along the two 0° layers that alternately bridged the lap and the strap, and the crack path was separated into two; arrester/lap interface and arrester/strap interface. Furthermore, the 90°

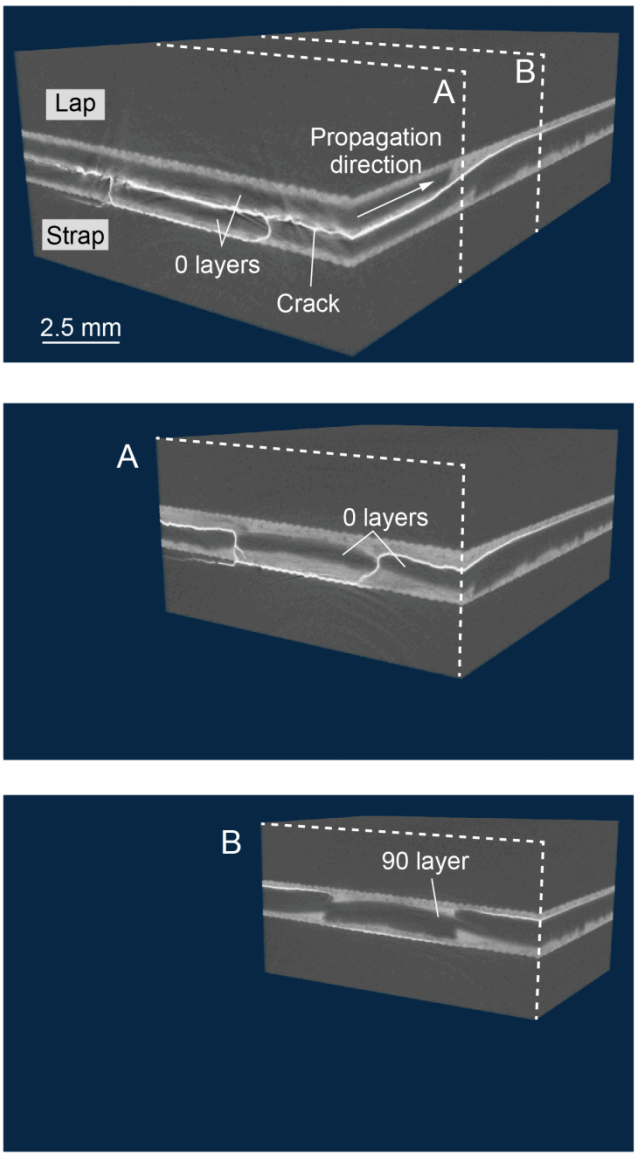

Figure 5: X-ray CT image of 0-3_90-2 specimen.

layer bridged the two crack paths and constrained the separation of the lap and the strap (cross-section B). It should be noted that fiber breakage was not observed in both 0° and 90° layers, confirming that carbon/epoxy prepreg is a suitable material for arresting fatigue crack.

3 FINITE ELEMENT ANALYSIS TO UNDERSTAND MECHANISM

Finite element models with 5mm width were made using Abaqus 6.14 by taking account of the periodicity of the arrester in the specimen width direction, and the stress-strain state was calculated when a load of 15kN was applied. The arrester part was modeled based on the configuration of Specimen 0-1_90-1 (Fig. 6) and a 40mm long crack was introduced in the model (i.e., the crack passes through the arrester crossing part by 10mm). Energy release rates at the crack tip were calculated using the virtual crack closure technique (VCCT) [5].

Figure 7 presents the energy release rate calculated. In the case without the arrester, mixed-mode deformation was induced around the crack tip and mode-II was dominant. In contrast, by introducing the arrester, the mode-I crack-opening deformation was completely suppressed and mode-II energy release rate decreased by 70%. Figure 8 shows the deformation around the crack tip calculated by FEA. In the model without the arrester, tensile deformation of the strap part, opening of the crack, and secondary bending deformation due to the eccentric load path between the strap and the overlap part occurred, resulting in mixed-mode deformation around the crack tip. In contrast, in the model with the arrester, the 90° layer constrained by the two 0° layers bridged the crack, suppressing opening of the crack and the secondary bending deformation. Both mode-I and mode-II energy release rates decreased (Fig. 7) and, as a result, the crack growth rate in the CLS fatigue test decreased after the crack tip passed through the crossing part of the arrester.

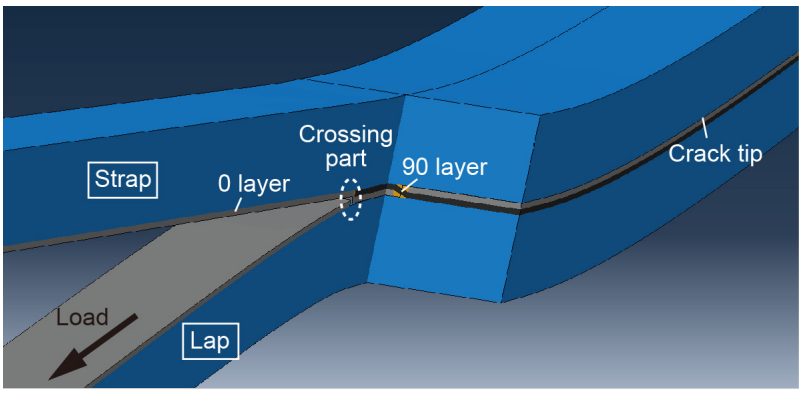

Figure 6: Finite element model with crack arrester.
Arrester part was modeled based on configuration of Specimen 0-1_90-1

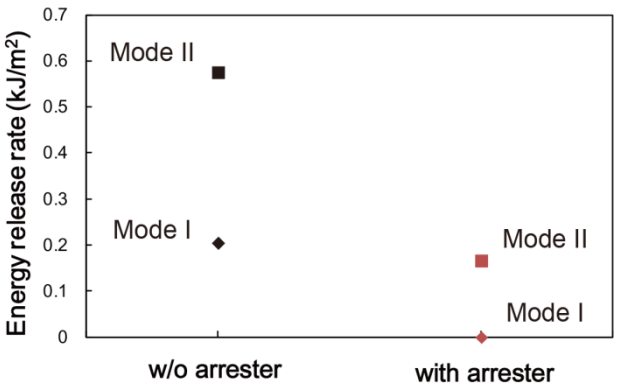

Figure 7: Reduction of energy release rate by crack arrester.

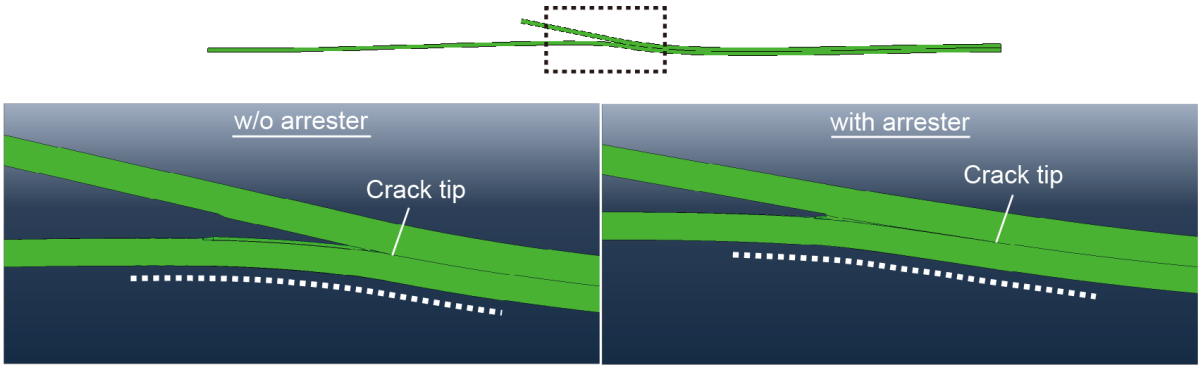

Figure 8: Deformation near crack tip. Arrester 90° layer constrained by 0° layers suppresses crack opening and secondary bending deformation, resulting in reduced energy release rate.

4 CONCLUSIONS

This study evaluated the performance of the fiber-reinforcement-based crack arrester under fatigue loading conditions. CLS fatigue tests simulating a loading condition near stiffener run-out were conducted and the crack propagation behavior was observed. The crack growth speed dramatically slowed down after the crack tip passed through the crossing part of the arrester and the reduction rate depended on the arrester thickness. In addition, FEA was conducted to understand the arresting mechanism and it was clarified that the suppression of crack opening and secondary bending was the key mechanism of the crack stopping.

ACKNOWLEDGEMENTS

This work was supported by JSPS KAKENHI, Grant Number 17H03475.

REFERENCES

[1] Kruse, T. (2013). Bonding of CFRP primary aerospace structures: overview on the technology status in the context of the certification boundary conditions addressing needs for development. *Proceedings of The 19th International Conference on Composite Materials*, 5635-5643.

[2] S. Minakuchi. (2015). Fiber-reinforcement-based crack arrester for composite bonded joints. P*roceedings of The 20th International Conference on Composite Materials*, 2118-4.

[3] S. Minakuchi and N. Takeda. (2016). Arresting crack in composite bonded joint using fiber-reinforcement-based design feature. *Proceedings of 17th European Conference on Composite Materials*, WED-1_STO_3.20-03.

[4] T. Kruse, T. Körwien, S. Heckner and M. Geistbeck. (2015). Bonding of CFRP primary aerospace structures – crackstopping in composite bonded joints under fatigue. *Proceedings of The 20th International Conference on Composite Materials*, 2219-1.

[5] Krueger, R. (2004). Virtual crack closure technique: history, approach, and applications. *Applied Mechanics Reviews*, 57(2), 109-143.